JBUON 2015; 20(4): 1154-1163
ISSN: 1107-0625, online ISSN: 2241-6293 • www.jbuon.com
E-mail: editorial_office@jbuon.com

ORIGINAL ARTICLE

Stereotactic body radiation therapy patient specific quality assurance using a two-dimensional array at extended source to surface distance

Sotirios Stathakis[1], Panayiotis Mavroidis[1], Ganesh Narayanasamy[1], Miljenko Markovic[1], Pamela Myers[2], Niko Papanikolaou[1]

[1]*Department of Radiation Oncology, University of Texas Health Sciences Center at San Antonio, TX, USA;* [2]*Department of Radiation Oncology. Baylor College of Medicine, Houston TX, USA*

Summary

Methods: *Five patients with 38 fields have been analyzed in this study. The plans were optimized for the following clinical sites: one liver, one lung, one brain, one prostate and one spine. The detector array used for the measurements was the PTW Seven29 array. All the plans were optimized and calculated using Eclipse v8.9. The center of the array was setup at 215 cm from the source and all the fields were measured and analyzed one by one. All the 30 measurements were performed on a NovalisTX linear accelerator equipped with a high definition multileaf collimator. The evaluation was based mainly on gamma index passing rates using 2 mm distance to agreement (DTA) and 2% dose difference.*

Results: *The accuracy of the Eclipse Treatment Planning System (TPS) at extended Source to Surface Distances (SSDs) using an ionization chamber was measured to be within 1.0%. All the field measurements were performed and analyzed 35 individually. The percent of the points that had a gamma index of less than 1 using 3%/3 mm was >99% for all the measurements. In order to better evaluate our process and distinguish smaller differences a new set of results was obtained by applying gamma index tolerances of 2%/2mm. In this case, the gamma index passing rates ranged from 90.8 to 100% (95.5%±3%). The profile comparison showed that the detector array measurements followed closely the calculated 40 profiles, even for fields optimized with multiple peaks and valleys.*

Conclusion: *The choice of the IMRT QA device has an important role in the results of the patient specific QA of the delivered dose to the patient in the case of small targets as in the treatment of spinal targets. In this study, we demonstrated that an extended SSD measurement can improve the sampling resolution of a two-dimensional (2D) detector array, in our case the PTW 45 Seven29 array. This method was shown to be accurate and efficient for measuring highly modulated small fields for pre-treatment patient specific QA.*

Key words: *DQA, IMRT, measurements at extended SSD, SBRT*

Introduction

2D ionization chamber arrays are widely used in the clinical setting for the pre-treatment verification of IMRT plans. However, the sampling resolution of such arrays has been shown to degrade the accuracy of the measurement, especially for small, highly-modulated fluence maps that are typical of SBRT fields [1-3].

The pre-treatment QA measurements for these fields frequently fail due to the poor sampling of the delivered dose distribution by the ar-

Correspondence to: Sotirios Stathakis, PhD. Department of Radiation Oncology, University of Texas Health Sciences Center at San Antonio, TX 78229, USA. Tel: +1 210 450 1010, E-mail: Stathakis@uthscsa.edu
Received: 27/10/2014; Accepted: 14/11/2014

ray as defined by the Nyquist criteria. Film dosimetry, whether it is using an extended range film requiring wet chemistry, or an organic monomer film such as the gafchromic film, offers high spatial resolution but has its own challenges [4-6]. Given the popularity of the 2D arrays, stemming primarily from their ease of use, absolute calibration, instantaneous readout and efficiency, we have conducted this study to examine the effects of an extended SSD measurement technique on chamber array resolution and the application of such technique for small field IMRT dosimetry [7-10].

For a 2D detector array with a given spatial resolution, a number of methods can be used to effectively increase the number of detectors that sample the measurements. First, one can obtain multiple measurements by shifting the array at discrete steps and then combining the measurements into one summed distribution. Second, one can perform measurements at an extended SSD thereby increasing the number of detectors that sample the dose distribution due to the divergence of the beam with increasing distance from the radiation source. The first method increases the time required for QA and there is some uncertainty associated with each shift of the array. In the second method, the time for QA does not increase, but there is some uncertainty associated with the dose calculation from the TPS due to the modeling of the beam at extended SSD [11]. Our investigation aims to explore the 78 feasibility of using the extended SSD method as a means to accurately and adequately sample the dose distribution from small IMRT fields for the purpose of pre-treatment dose verification.

Methods

The PTW OCTAVIUS II (PTW Freiburg, Germany) system was used in this study. The system consists of the OCTAVIUS phantom and the 2D Seven29® detector array. The array has a resolution of 1 cm center-to-center and consists of 729 parallel plate vented 86 ionization chambers arranged over an area of 27x27 cm (Figure 1).

The measurements were obtained at a distance of 215 cm Source to Array Distance (SAD) which corresponds to an SSD of 199 cm (the radius of the phantom is 16 cm). The SAD is the distance from the target to the center of the detector array when the phantom is placed on the floor (Figure 1A). Measurements were also made at the same distance with the array on the table (Figure 1B) to investigate the effect of backscatter from the concrete floor. For those measurements, the phantom was placed on its side on the treatment couch, and the gantry was rotated to 90° so that the beam is perpendicular to the detector array, reproducing in essence the geometry from Figure 1A in the absence of floor scatter.

The dose calculation accuracy of the Eclipse (ver. 8.9, Varian Medical Systems, Palo Alto, CA) TPS was evaluated at the extended distance of 215 cm, using point measurements in the phantom by means of an ionization chamber (PTW TN31010). The ionization chamber dose measurements were compared to the values calculated by the Eclipse TPS.

The measurements consisted of a pyramid field (composed of overlapping 1x1, 2x2, 3x3, 5x5, and 10x10 cm^2 fields) and 38 fields from 5 SBRT plans. The planar doses were also calculated with the Eclipse TPS for the same beams, using the CT scan of the OCTAVIUS II phantom. The evaluation of the measurements was performed using gamma index analysis and profile comparisons between the measurements at each SAD against the calculated planar doses [12-14]. For the gamma index passing rate calculation, the criteria were set to 3% dose difference and 3 mm DTA. The gamma index analysis was repeated using a 2%/2 mm criterion to further challenge the application of the proposed method (Table 1).

Results

TPS accuracy and backscatter from the floor

The Eclipse TPS was evaluated for its dose calculation accuracy at extended SSD. The dose to the center of the OCTAVIUS II system was measured using a PTW TN31010 ionization chamber. The monitor units to deliver 1.0 Gy and 2.0 Gy to the effective point of measurement in the ionization chamber were calculated using Eclipse. The dose measured was within 1% of the Eclipse calculated value. A dose plane evaluation of open fields (10x10, 5x5 and 2x2 cm^2) using the detector array showed very good agreement between Eclipse and measured dose. An example of the agreement is shown in Figure 2.

The next test was designed to investigate whether the measurement accuracy would be affected by the placement of the phantom on the floor due to back scatter. The dose measured with the ionization chamber on the floor (Figure 1A) was compared against the corresponding measurements when the phantom was placed on the treatment couch at the same distance (Figure 1B). There was no difference observed between the two measurements for the same irradiation geometry and the same number of monitor units (MUs).

Patient measurements

The small fields/segments measurements

Table 1. Field characteristics for each plan measured (the gantry angles are in Varian coordinate system)

Site	*# beams*	*MU*	*Gantry angle (couch angle)*
Lung	8	191, 188, 249, 236, 189, 149, 148, 347	60(195), 80(170), 118(185), 146(160), 200(111), 230, 170, 25
Liver	9	285, 389, 253, 346, 667, 254, 284, 251, 269	20, 315, 250, 190, 160, 220(195), 280(195), 270(165), 300(165)
Brain	7	60, 165, 147, 198, 288, 120, 309	330, 300, 260, 322, 10, 236, 42
Prostate	7	69, 82, 57, 70, 63, 65, 63	330, 280, 230, 180, 130, 80, 30
Spine	7	654, 602, 574, 624, 646, 617, 426	330, 280, 230, 130, 80, 30, 0

using the OCTAVIUS II system at 100cm SAD, showed that the number of detectors inside the field outline was very limited. Figure 2 shows that a small number of all available detectors are used in the gamma index calculations, and that the profile is not resolved accurately. The gamma index passing rate in those cases was generally high (>99%). However, it is clear from the planar dose distribution and profiles (Figure 2) that the spatial resolution of the detectors is not adequately sampling the dose distribution. As it can be seen in Figure 3, the detector array can accurately measure the dose at the detector locations but fails to resolve the shape of the profile (Figure 3 top right).

Results similar to the ones shown in Figure 3 were observed for the majority of the fields we tested. The average gamma index passing rate was above 99%. The low number of detectors used for the measurements cannot effectively resolve the profiles accurately, since the peaks and valleys of the dose distributions are not resolved as a result of the limited inherent spatial resolution of the detector array.

The first extended SSD experiment was for the pyramid field that provided a controlled environment to test our hypothesis. The comparison of the measured and calculated planar doses in the phantom at the level of the detectors is shown in Figure 4. Note that the number of dose points evaluated is 479 out of the possible 729 (65.7%) while for the same measurement at 100 cm SAD only 100 dose points were evaluated (13.7%). The gamma index passing rate for the extended SSD using 3% and 3 mm criteria is 100.0%.

Each SBRT patient field was measured and

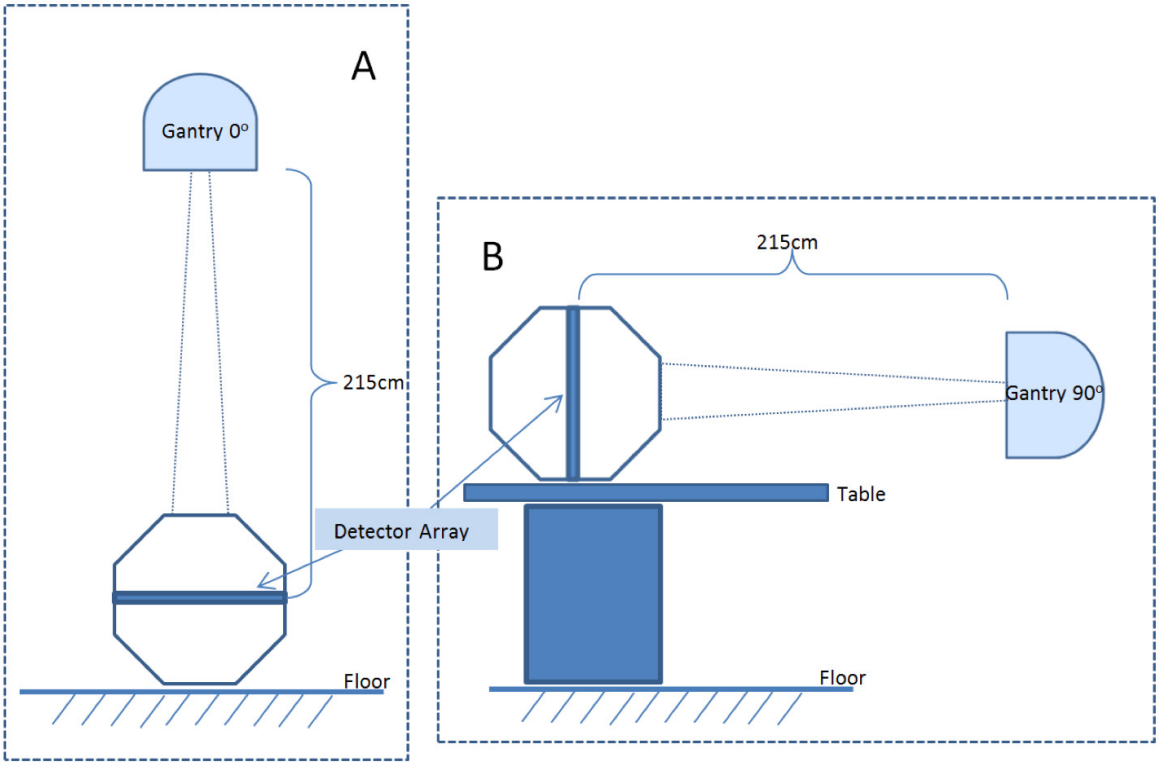

Figure 1. Setup geometry of the detector array when placed on the floor **(A)** and on the treatment couch **(B)**. The dashed line represents the plane of the measurement in the array which corresponds to the calculation plane extracted from the TPS.

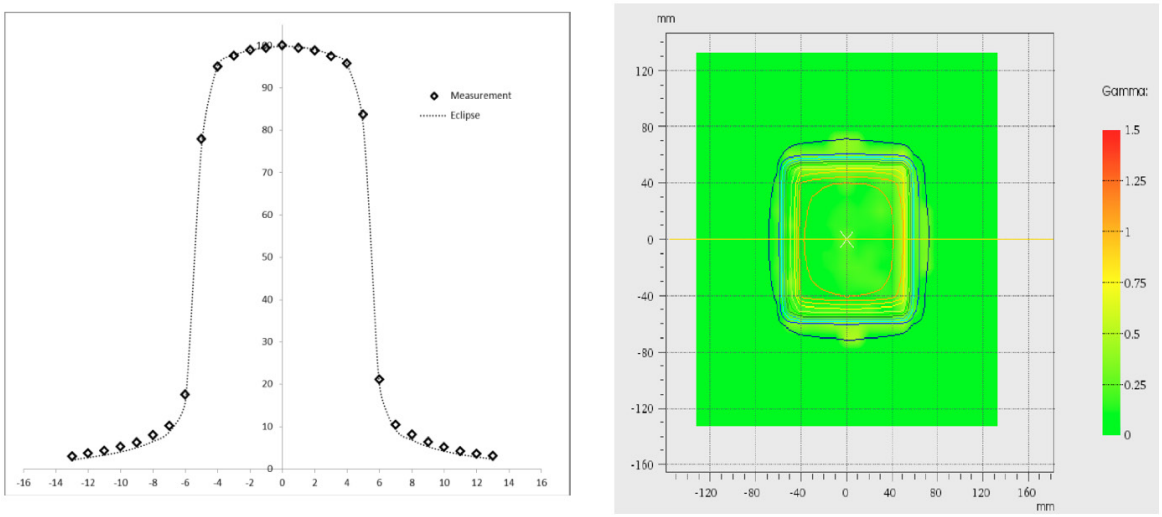

Figure 2. Cross line profile comparison (left) and 3mm/3% (right) between measurements and Eclipse predicted dose distribution at the plane of the detector array for a 5x5 cm^2 field irradiated at 215 cm SDD.

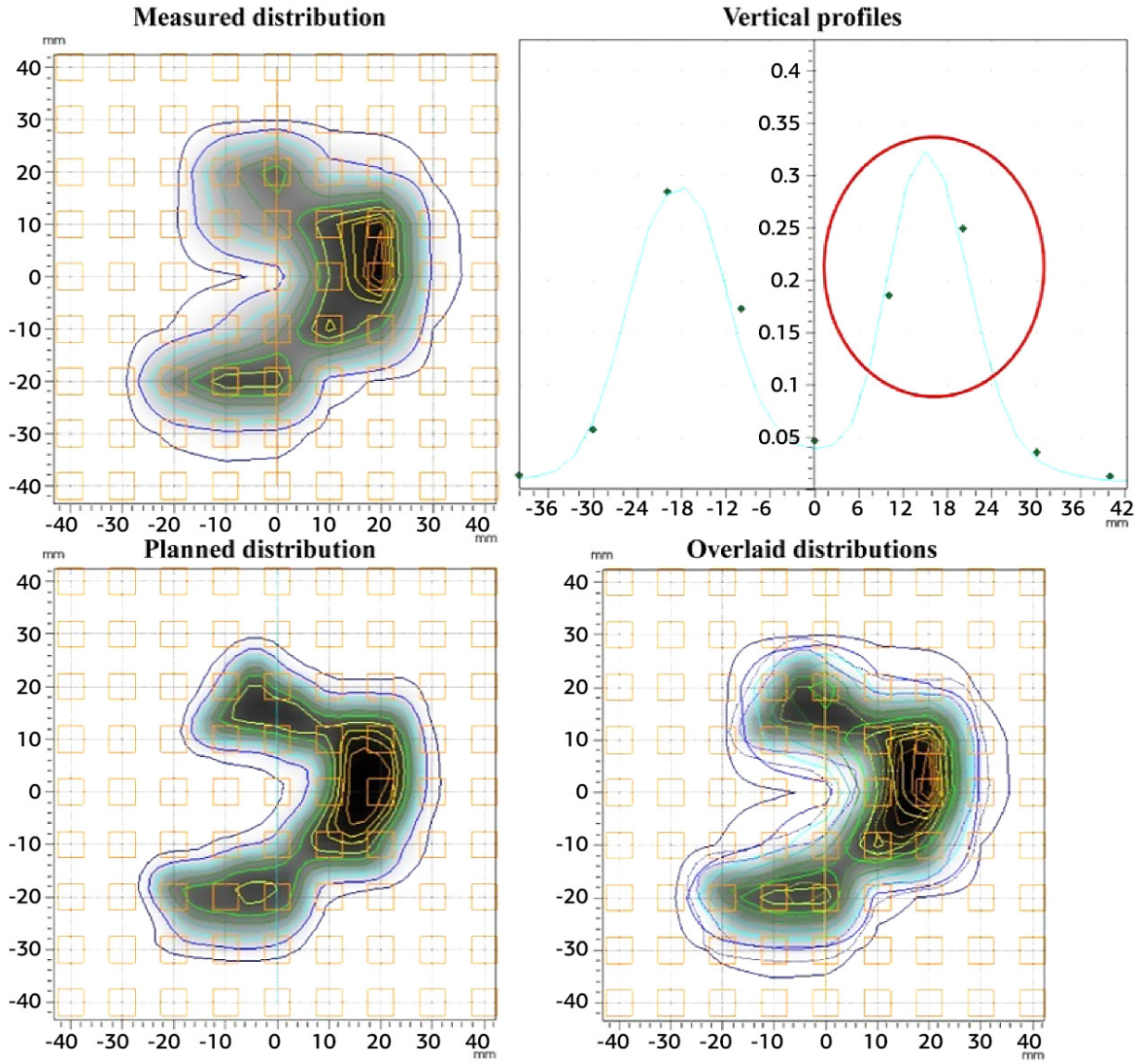

Figure 3. Comparison of measured and calculated planar doses at 100 cm SAD. The detector locations are overlaid on the dose distributions. The top right quadrant shows a vertical profile (comparison through the center of the detector array). The line represents the planned dose profile whereas the dots represent the measurements of the detectors.

Table 2. The gamma indices for the clinical plan analysis at 100 cm and 215 cm SAD

	100 cm		*215 cm*		*Difference*	
Site	*3%/3 mm*	*2%/2 mm*	*3%/3 mm*	*2%/2 mm*	*3%/3 mm*	*2%/2 mm*
Brain	94.4	94.4	100.0	96.5	5.6	2.1
	100.0	100.0	100.0	97.9	0.0	-2.1
	100.0	100.0	100.0	90.7	0.0	-9.3
	100.0	95.5	100.0	92.1	0.0	-2.9
	100.0	100.0	100.0	99.1	0.0	-0.9
	100.0	100.0	100.0	96.0	0.0	-4.0
	100.0	96.4	100.0	98.2	0.0	1.8
Liver	100.0	94.8	100.0	98.5	0.0	3.7
	100.0	100.0	100.0	100.0	0.0	0.0
	100.0	97.6	100.0	100.0	0.0	2.4
	100.0	100.0	100.0	97.2	0.0	-2.8
	100.0	98.2	100.0	97.8	0.0	-0.4
	100.0	98.1	100.0	96.7	0.0	-1.4
	100.0	100.0	100.0	100.0	0.0	0.0
	100.0	97.7	100.0	97.8	0.0	0.1
	100.0	100.0	100.0	100.0	0.0	0.0
Lung	86.4	81.8	100.0	87.6	13.6	5.8
	100.0	100.0	98.7	92.2	-1.3	-7.8
	100.0	92.0	100.0	99.1	0.0	7.1
	100.0	92.0	100.0	95.7	0.0	3.7
	100.0	95.0	100.0	100.0	0.0	5.0
	100.0	92.0	100.0	96.4	0.0	4.4
Prostate	97.9	95.8	100.0	86.4	2.1	-9.1
	97.9	93.6	100.0	94.0	2.1	0.4
	97.9	95.7	95.0	94.0	-2.9	-1.7
	100.0	91.7	97.2	86.7	-2.8	-5.0
	100.0	91.7	98.7	94.4	-1.3	2.7
	100.0	91.7	100.0	95.8	0.0	4.1
	100.0	95.7	100.0	95.9	0.0	0.2
Spine	90.5	76.2	100.0	99.2	9.5	23.0
	92.3	84.6	100.0	97.0	7.7	12.4
	92.3	79.5	99.3	95.5	7.0	16.0
	92.3	84.6	100.0	96.4	7.7	11.8
	95.2	83.0	99.3	95.2	4.1	12.2
	95.2	76.2	100.0	95.8	4.8	19.6
	97.5	80.0	99.1	97.4	1.6	17.4
Mean	98.1	92.9	99.6	95.9	1.6	3.0

analyzed individually (Table 1). This Table shows the gamma index values calculated after the analysis of field using two sets of gamma index criteria. First, the comparison of measurements and calculations was performed using the 3% dose difference and 3 mm DTA criteria while suppressing the doses below 10% of the maximum dose measured for each field to remove the noisy part of the distribution. The number of dose points measured for each field was nearly four times larger in the extended SSD measurements (Figure 5 vs Figure 3), and the gamma index using 3%/3 mm ranged from 95.0 to 162 100.0% with an average of 99.6%. At the same time, the same fields, when measured at 100 cm SAD had gamma index values between 86.4 to 100.0% with an average of

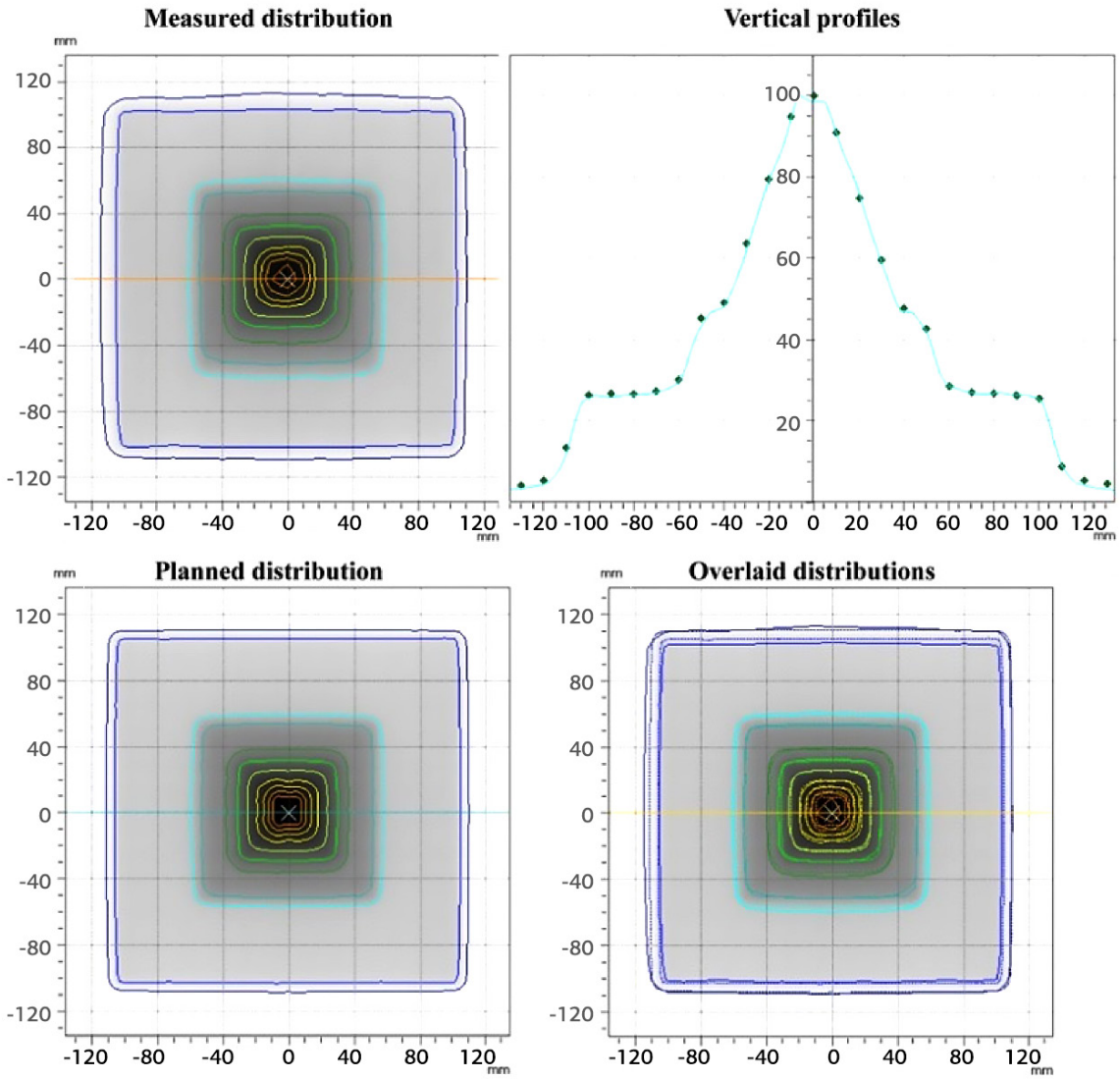

Figure 4. Comparison of the planar doses between the TPS calculated and measurement of a jaw-defined pyramid dose distribution at 215 cm SAD.

98.1%. To better evaluate this technique and to reveal smaller differences, a new set of gamma index criteria was used by employing the 2%/2 mm criteria. The gamma index for these gamma index parameters 166 ranged from 86.7-100% (average 95.9%) for the 215 cm SAD measurements and from 76.2-100.0% (average 92.9%) for 100 cm SAD (Figure 5). The profile comparison showed that the detector array measurements could accurately resolve the calculated profiles, even in fields that contained multiple peaks and valleys (Figure 4).

The gamma indices for the clinical plan analysis at 100 cm and 215 cm SAD are shown in Figure 6. The analysis was performed using 3%/3 mm and 2%/2 mm gamma analysis criteria. The data is also tabulated in Table 2.

Discusion

An extended literature review has revealed only one publication [15] on the topic of dose measurements at extended SSD. More specifically, no published data was published on patient specific measurements at extended distances.

The challenge of dosimetric verification for small fields, such as those often used in SBRT, is the size of the beam aperture, especially for IMRT deliveries where the constituent segments producing the intensity modulation are even smaller. QA of such fields is challenging, in particular when it is conducted using 2D detector arrays due to their low sampling resolution. Film could be used in such instances to take advantage of its high spatial resolution. However, the develop-

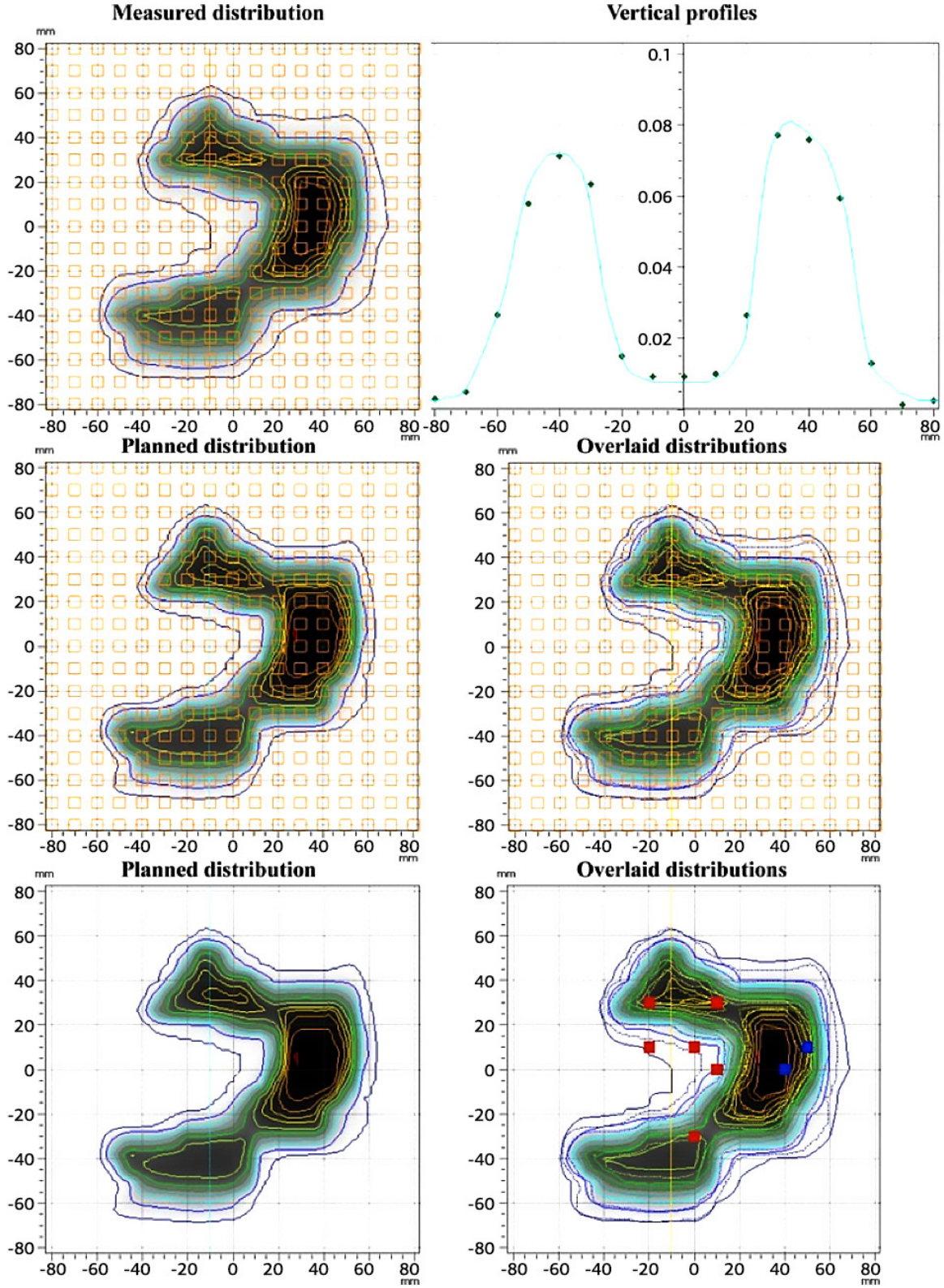

Figure 5. Comparison of measured and calculated dose distributions using the 3% dose difference and 3mm DTA (top two rows) and the 2% dose difference and 2 mm DTA (bottom row) criteria.

ment, scanning and calibration of the film, introduce sources of error and, overall, the measurement and analysis process is not as efficient as that of a 2D detector array.

The method we propose has the advantage of using a single measurement while at the same time increasing the number of measuring points by a factor of 4. By setting up the detector at a

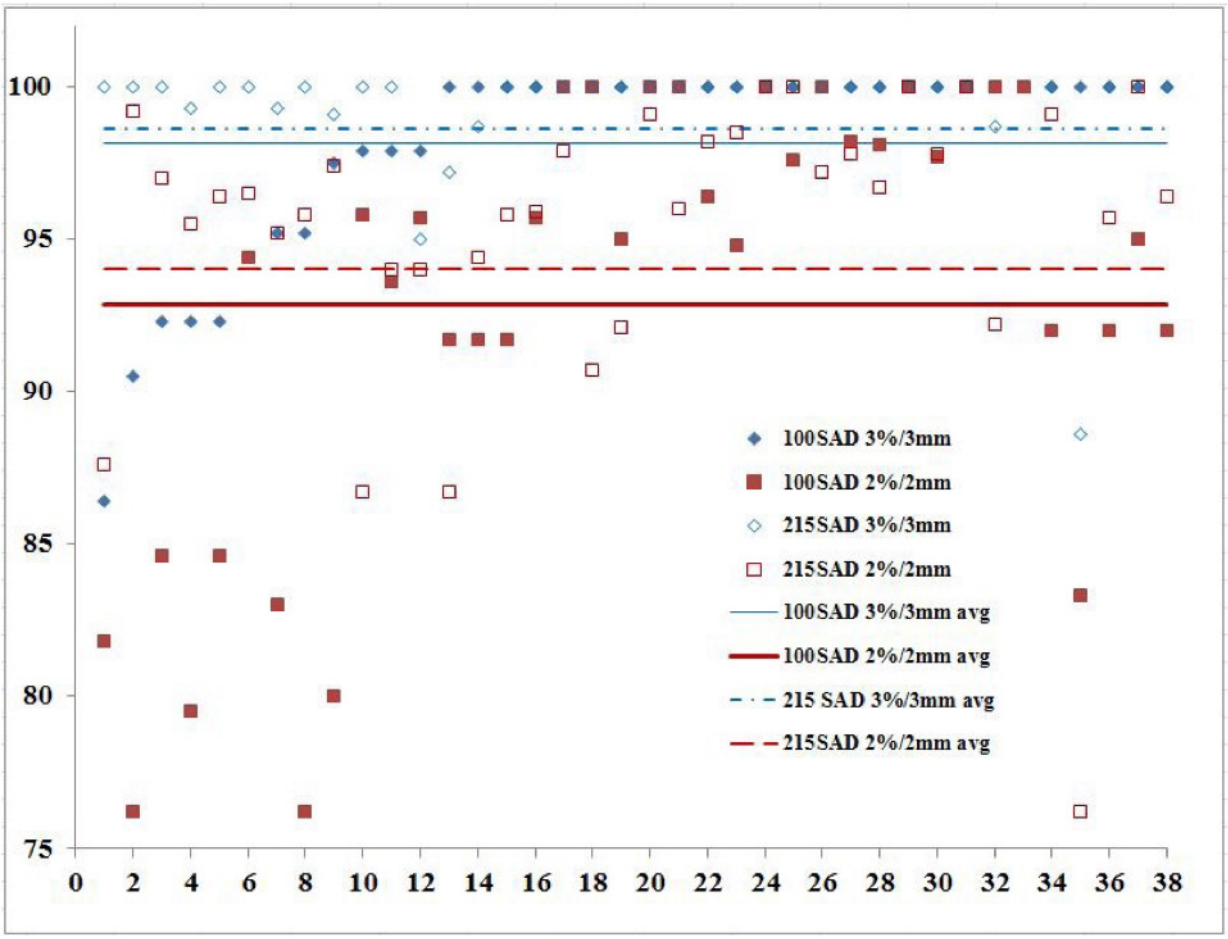

Figure 6. Shown above are the gamma indices of the 38 clinical IMRT beams. Solid symbols represent the results at 100 cm SAD and outlined symbols represent 215 cm SAD using 3%/3 mm and 2%/2 mm, respectively.

distance of approximately 2 meters from the source, the irradiated area for each field increases by a fourfold, and consequently the number of detectors inside the radiation field increases by the same amount. Similar results have been reported by Tierney et al. [15]. They have reported a 4.8 increase of the sampling points with the use of the IBA MatriXX at a distance of 208 cm.

Gamma criterion with 3%/3 mm for the comparison of the measured and calculated data has been accepted and widely used. If, for the moment, we eliminate intrinsic characteristics of the single detector and 2D detector array, numerical percentage of passing rate highly depends on the number of sampling points. While increasing the number of points with extended distance we can get better spatial representation of the measured fluence map, but this does not necessarily lead to increase in percentage passing rate. The sampling frequency of the detector (0.1/mm) stays the same with extended distance and for the highly modulated fields the gamma criterion 2%/2 mm could yield the similar numerical percentage-passing rate as isocentric measurements. Dose grid 204 resolution for fluence map optimization [16] for highly modulated fields is <2.5 mm spacing that would require higher sampling frequency (preferable 0.4/mm). The proposed method increases the number of sampling points. It is worth mentioning that computing of the gamma function [17] using original evaluated dose points in a one-dimensional distribution or geometric distance from the normalized reference point to the normalized evaluated distribution dose curve contributes to the numerical percentage passing rate as well. Comparison using different gamma criteria should be accepted as a tool with limitations when it comes to sampling frequency and spatial resolution.

Lack of lateral charge particle equilibrium,

steep dose gradient, detector volume averaging, occlusion of the direct photon beam source, collimator settings, beam energy and penumbra are challenges in the small field dosimetry measurements [18,19]. Comparison of discrete measured values with the calculated continuous values emphasizes the importance of sampling frequency (Nyquist theorem). The size of the detector, intrinsic characteristics as well as detector's composition greatly influences the measurements. The volume effect of detectors and positioning accuracy [20] are also affecting the accuracy of the profiles in the penumbra region. With extended distance we couldn't avoid the presence of volume averaging effect [21,22] as well as the lateral response function of the single detector, which are shown to be important characteristics in the dosimetry of highly modulated small beams that lack the charge particle equilibrium.

The dose rate at the extended distance is significantly reduced and so it is important to use a detector array that has no dose rate dependence. The commercially available ion chamber arrays show minimum dose rate dependence in a linear response for changes between 100 cm and 200 cm SSD. The penumbra will also increase as the SSD increases and will affect the measurement. However, if the planning system can accurately calculate the dose at extended SSD, the comparison between measurement and calculation is valid. Most modern TPS have a convolution/superposition type dose engine that can accurately predict the dose at extended distances. Our TPS was tested for its accuracy at an extended SSD against a calibrated chamber and was found to be in agreement within 1%.

Conclusion

In this study, we demonstrated that an extended SSD measurement could increase the number of sampling points of a 2D detector array, in our case the PTW Seven29 array. This method was shown to be accurate and efficient for measuring highly modulated small fields for pre-treatment patient specific QA.

References

1. Poppe B, Blechschmidt A, Djouguela A et al. Spatial resolution of 2D ion chamber arrays for IMRT dose verification: single detector size and sampling step width. Phys Med Biol 2007;52:2921-2935.
2. Galvin JM, Bednarz G. Quality assurance procedures for stereotactic body radiation therapy. Int J Radiat Oncol Biol Phys 2008;71:S122-S125.
3. Webb S (Ed). Intensity Modulated Radiation Therapy Institute of Physics Publishing, Bristol, UK (2000).
4. Sorriaux J, Kacperek A, Rossomme S et al. Evaluation of Gafchromic (R) EBT3 films characteristics in therapy photon, electron and proton beams. Phys Med 2013;29:599-606.
5. Borca VC, Pasquino M, Russo G et al. Dosimetric characterization and use of GAFCHROMIC EBT3 film for IMRT dose verification. J App Clin Med Phys 2013;14:158-171.
6. Ju SG, Han Y, Kum O et al. Comparison of film dosimetry techniques used for quality assurance of intensity modulated radiation therapy. Med Phys 2010;37:2925-2933.
7. Poppe B, Blechschmidt A, Djouguela A et al. Two-dimensional chamber arrays for IMRT plan verification. Med Phys 2006;33:1005-1015.
8. Li S, Rashid A, He S et al. A new approach in dose measurement and error analysis for narrow photon beams (beamlets) shaped by different multileaf collimators using a small detector. Med Phys 2004;31:2020-2032.
9. Martens C, Wagter C, De Neve W et al. The value of the LA48 linear ion chamber array for characterization of intensity-modulated beams. Phys Med Biol 2001;46:1131-1148.
10. Spezi E, Angelini AL, Romani F et al. Characterization of a 2D ion chamber array for the verification of radiotherapy treatments. Phys Med Biol 2005;50:3361-3373.
11. Fraass B, Doppke K, Hunt M et al. American Association of Physicists in Medicine Radiation Therapy Committee Task Group 53: quality assurance for clinical radiotherapy treatment planning. Med Phys 1998;25:1773-1829.
12. Low DA, Harms WB, Mutic S et al. A technique for the quantitative evaluation of dose distributions. Med Phys 1998;25:656-661.
13. Tsai JS, Wazer DE, Ling MN et al. Dosimetric verification of the dynamic intensity modulated radiation therapy of 92 patients. Int J Radiat Oncol Biol Phys 1998;40:1213-1230.
14. Boehmer D, Bohsung J, Eichwurzel I et al. Clinical and physical quality assurance for intensity modulated radiotherapy of prostate cancer. Radiat Oncol 2004;71:319-325.
15. Tierney K, Morales M, Coffey C et al. Improvements to Ion Chamber Array Spatial Resolution at Extended SSD. Med Phys 2012;39:3716.
16. Dempsey JF, Romejin HE, Li JG et al. A Fourier analysis

of the dose grid resolution required for accurate IMRT fluence map optimization. Med Phys 2005;32:380-388.

17. Ju T, Simpson T, Deasy JO et al. Geometric interpretation of the gamma dose distribution comparison technique: Interpolation-free calculation. Med Phys 2008;35:879-886.
18. Sharpe MB, Jaffray DA, Battista JJ et al. Extrafocal radiation: A unified approach to the prediction of beam penumbra and output factors for megavoltage x-ray beams. Med Phys 1995;22:2065-2074.
19. Das IJ, Ding GX, Ahnesjo A. Small fields: Nonequilibrium radiation dosimetry. Med Phys 2008;35:206-215.
20. Swanpalmer J, Johansson KA. The effect of air cavity size in cylindrical ionization chambers on the measurements in high-energy radiotherapy photon beams-an experimental study. Phys Med Biol 2012;57:4671-4681.
21. Markovic M, Stathakis S, Mavroidis P et al. Characterization of a 2-dimensional liquid-filled ion chamber detector array used for verification of the treatments in radiotherapy. Med Phys 2014;41:051704.
22. Bouchard H, Seuntjens J. Ionization chamber-based reference dosimetry of intensity modulated radiation beams. Med Phys 2004;31:2454-2465.